Fast Protection Strategy for DC Transmission Lines of MMC-based MT-HVDC Grid*

Sihua Wang[1, 2], *Lijun Zhou*[1, 2*], *Tian Wang*[1, 2], *Tianyu Chen*[1, 2] *and Yu Wang*[1, 2]
(1. College of Automation & Electrical Engineering, Lanzhou Jiaotong University, Lanzhou 730070, China;
2. Rail Transit Electrical Automation Engineering Laboratory of Gansu Province,
Lanzhou Jiaotong University, Lanzhou 730070, China)

Abstract: Multi-terminal high voltage DC (MT-HVDC) grid has broad application prospects in connecting different energy sources, asynchronous interconnection of power grids, remote load power supply, and other fields. At present, the key technologies that affect the development of MT-HVDC transmission system include swift fault identification and location in the DC line and its rapid isolation. Traditional fault monitoring relies on line communication, which cannot guarantee the rapidity and reliability of protection; moreover, it may even cause device damage. A fault identification scheme based on a single-terminal transient is presented in this paper. This scheme calculates the line inductance by using the rise rate of fault current at the initial stage of the fault, and determines the occurrence of the fault by comparing the observed line inductance with the set value, which lays a foundation for calculating the location of the fault point using distance protection. A simulation model on the PSCAD/EMTDC platform is built; the simulation example verifies that the proposed scheme can identify faults under dissimilar conditions while maintaining a low error level on the premise of no communication lines so as to meet the protection requirements of the MT-HVDC grid.

Keywords: Multi-terminal high voltage DC (MT-HVDC) grid, modular multilevel converter (MMC), DC circuit breaker (DCCB), bipolar short-circuit, fault identification

1 Introduction

High voltage DC (HVDC) transmission technology uses voltage source converter (VSC) as its core component and pulse width modulation (PWM) as its basic control theory. Its advantages when compared with the traditional AC transmission technology, are as follows: no risk of phase conversion failure and reactive power compensation problem, lower harmonic level and a smaller footprint. Owing to continuous development of power electronics technologies, HVDC transmission has become an important means of energy transport. The modular multilevel converter (MMC) was first presented in 2001 by a German scholar Rainer Marquardt [1]. Compared to the two- or three-level VSCs, MMCs provide benefits such as decreased losses, easier manufacturing, higher waveform quality, and increased fault removal capability. Accordingly, several MMC-HVDC grids have been completed, including multi-terminal HVDC (MT-HVDC) projects such as the Nan'ao three-terminal HVDC grid and the Zhoushan five-terminal HVDC grid. Moreover, the Zhangbei ±500 kV flexible HVDC project will be put into operation in 2020, this project is not only a large complex of wind, light, storage and other clean energy generation and storage mechanisms that employs HVDC power transmission, but it will also be the DC grid project with the highest voltage level, and hence, the largest transmission capacity worldwide [2-3].

Based on the characteristics of the current DC power grid, such as large transmission capacity and extended transmission distance, the MT-HVDC grid exhibits an immense potential in the field of urban power grids. At present, the MT-HVDC power grid mostly adopts the DC overhead line transmission and the topological structure of "half-bridge sub-module +

Manuscript received January 8, 2020; revised June 30, 2020; accepted August 6, 2020. Date of publication June 30, 2021; date of current version June 7, 2021.
* Corresponding Author, E-mail: lijunzhou93@163.com
* Supported by the National Natural Science Foundation of China (51767014) and the Scientific and Technological Research and Development Program of the China Railway (2017J010-C/2017).
Digital Object Identifier: 10.23919/CJEE.2021.000018

high voltage DC circuit breaker (DCCB)" with various operation modes and a responsive control system. However, due to its rapid response, in case the DC line fails, the fault will quickly propagate through complex paths, which will have an irreversible impact on the stable operation of the entire DC power grid. Therefore, research on DC fault protection is of great significance for the MT-HVDC power grid.

Currently, research on the fault protection of MT-HVDC power grid focuses on AC side protection, converter station protection, and DC transmission line protection. Furthermore, when studying transmission line protection, we should focus on DC fault detection, fault location, and fault removal. In a DC transmission network based on voltage source converters, line faults are predominantly cut off by disconnecting the AC circuit breakers located at both ends of the converter stations [4]. In Refs. [5-9], different DC fault protection schemes were introduced for ensuring the safety of HVDC power grids. Specifically, Ref. [5] proposed eliminating the fault current of DC line by blocking the converter; however, directly blocking the converter station would lead to a deteriorated system reliability and a reduced transmission efficiency. Ref. [6] presented a protection strategy based on self-cleaning converter; however, it cannot guarantee an uninterrupted transmission of power during failure and is unsuitable for medium-and large-scale DC power grids. Ref. [7] proposed a method that utilizes transient energy information of high frequency current to judge in-region/out-of-region faults, but this scheme cannot judge the location of the fault. In Ref. [8], a longitudinal differential protection criterion based on a line boundary element was proposed to extract transient voltage at both ends of the line. However, this criterion requires the measurement of a double-ended quantity, which further requires the help of a communication line, thus resulting in a certain delay. In Ref. [9], a differential protection strategy was therefore proposed to realize fault detection and discrimination by extracting current values at both ends of the line; this method too requires communication lines, which sacrifices the rapidity of fault protection. Due to the intricate system topology of MT-HVDC power grid and the diversity of fault types, the implemented fault protection scheme must meet the expectations for selectivity, rapidity, reliability, and sensitivity.

Based on the structure and DC fault characteristics of an MT-HVDC power grid, this paper proposes a DC fault detection and discrimination strategy which only considers the single-ended quantity of a DC line as its criterion. This fault protection scheme uses the rise rate of fault current to calculate the inductance of the circuit in real-time, determines the occurrence of the fault by comparing this real-time inductance value with that observed during normal operation. Subsequently, the single-ended traveling wave information is used to derive the location of the fault point, after which, the DCCB set by the line protection clears the fault. In order to test the practicability of this protection scheme, a four-terminal HVDC power grid was built on the PSCAD/EMTDC simulation platform, and the DC line bipolar short-circuit fault was considered as an example. Through real-time measurement of the rise rate of the current in each line, the event of DC fault occurrence in the system was identified and discriminated.

2 DC fault analysis of MT-HVDC

2.1 Modular multilevel converter

The International Council on Large Electric Systems (CIGRE) named HVDC transmission technology as "Voltage Source Converter DC Transmission". Since the 1990s, the voltage source inverters commonly used in HVDC project have undergone a transition from two-level and diode-clamped three-level to modular multilevel. Unlike VSCs, a MMCs is not directly connected in series with multiple IGBTs; rather, it uses a sub-module (SM) cascade method, which has the advantages of lower converter loss, better waveform quality, and faster fault handling [10]. The basic topology of MMC is illustrated in Fig. 1. Each bridge arm contains N sub-modules and a series reactor L_0. Each phase unit contains an upper and a lower bridge arm.

As is shown in Fig. 1, the SMs of MMC adopt a half bridge structure; moreover, each SM contains two

IGBTs, two anti-parallel diodes, and an energy-storage capacitor. MMC supports the voltage of DC bus through the voltage U_c of each SM capacitor C_0.

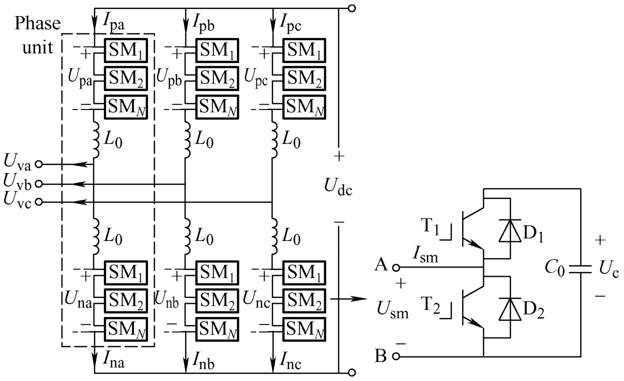

Fig. 1 Topological Structure of an MMC and its SM

2.2 Characteristic analysis of the DC short-circuit fault

There are three types of faults in DC transmission line of MT-HVDC power grid, namely: open circuit fault, unipolar ground fault, and bipolar short-circuit fault [11]. Considering the impact of these faults on the system, the occurrence of unipolar ground faults in HVDC transmission line is the most frequent. However, the damage it causes is far less than that incurred by a bipolar short-circuit fault; moreover, the rising speed of its fault current is slower than that of latter. Therefore, bipolar short-circuit faults cause the most severe damage. Furthermore, the variation trend of the characteristic quantity of the system after the occurrence of both these faults is similar; consequently, the detection scheme of one fault is also suitable for the other. Accordingly, this paper considers the bipolar short-circuit fault as an example to analyze the detection and location of HVDC line fault.

In the initial stage of this fault, the DC voltage drops rapidly; meanwhile, the main component of the fault current in the line is the capacitor discharge current of the inverter SM [12]. After a few milliseconds, the AC side also feeds short-circuit current to the fault point through the diodes of the SM, as depicted in Fig. 2. Moreover, because the fault current rises at an extremely fast speed, it can increase by several times, or even a dozen times, within a few milliseconds. Therefore, if the fault is not isolated in time, the power electronic devices may be affected.

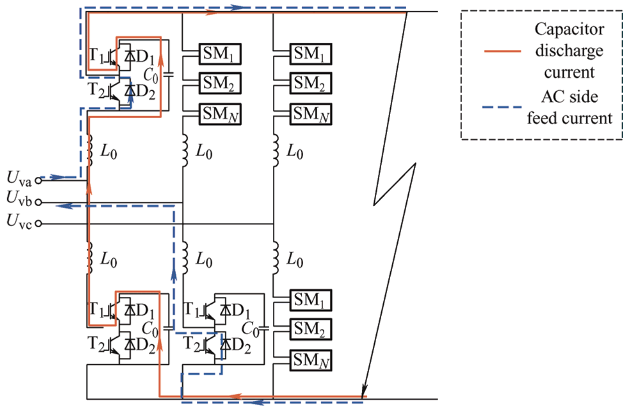

Fig. 2 Fault current path during a bipolar short-circuit fault

3 DC fault detection of MT-HVDC

3.1 Protection configuration on the DC side

The half-bridge MMC does not have fault self-cleaning capability; therefore, it is necessary to install DCCB on both sides of the DC line to remove the fault. Currently, three types of DCCBs are implemented in the HVDC transmission system, namely: mechanical, solid-state, and hybrid CBs. The hybrid DCCB comprises of the first two of these types and exhibits the following advantages: a short opening time, a large breaking current, and a low on-state loss [13]; it's hence more suitable for a flexible HVDC grid. Proposed by ABB in 2012, its typical topology is illustrated in Fig. 3, which consists of a current-carrying branch, a current-transfer branch, and an energy-absorption branch [14].

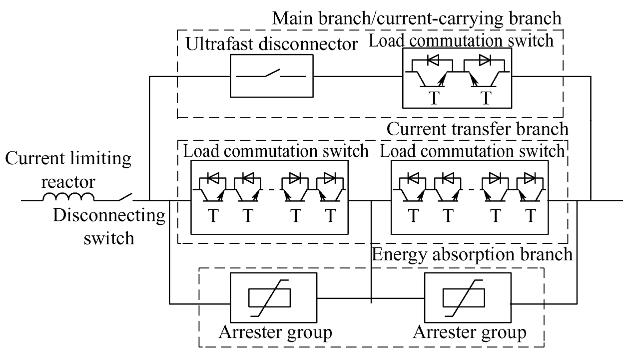

Fig. 3 Topology of a hybrid DCCB

During the steady-state operation, the current flows through the current-carrying branch, i.e., the ultrafast disconnector (UFD) and load commutation switch (LCS) are closed. When the DC line fails, the

LCS on the current-carrying branch is turned off, and the current hence flows through the current-transfer branch. After the UFD is switched off, the transfer switch in the current-transfer branch is disconnected, and the current is then transferred to the energy-absorption branch formed by the arrester group and is discharged to complete a fault current division. Since HVDC system has low damping; therefore, the fault current rises quickly and exhibits a larger amplitude when a short-circuit fault occurs. Taking Zhangbei project as an example, DC fault clearing time is recommended to be within 6 ms and the DCCB operating time is known to be approximately 3 ms [15]; therefore, the fault detection and location time must be less than 3 ms.

3.2 Fault detection principle based on the rise rate of the current

Commonly used types of protections mechanisms for DC lines of the HVDC grid include double-ended and single-ended protection. The former requires a communication channel to extract the voltage/current amount at both ends [16]. However, HVDC transmission systems often span long distances and are subjected to heavy loads and complicated environment along the line, which reduces the protection reliability, which further prolongs the protection time. Single-ended quantity-based protection avoids the problem of information volume exchange on both sides of the line. It is designed to measure the locally available information to detect the fault and locate the fault point. Therefore, researching and optimizing the single-ended quantity protection principle is an important aspect of HVDC grid fault protection.

The cooperation strategy of differential under-voltage protection and traveling wave protection is generally adopted as the main protection of DC lines in the HVDC transmission projects that have been brought into operation. However, setting up the former among these two is complex; moreover, it lacks theoretical analysis and calculation methods, and there exists the problem of insufficient sensitivity when the transition resistance is large [17-18]. Therefore a responsive protection strategy based on single-ended quantities of the line is proposed. After encountering a fault, it cooperates with the traveling wave protection mechanism to perform fault removal. HVDC power grids with a half-bridge "MMC+DCCB" structure are usually designed with the time-domain characteristic protection with DC voltage or current as its characteristic quantity. Considering the bipolar short-circuit fault current path, as depicted in Fig. 2, if the fault current fed by the AC-side power supply is ignored, the path can be simplified. Accordingly, the equivalent circuit, when the capacitors of the SM are discharged, at the initial stage of the fault is illustrated in Fig. 4.

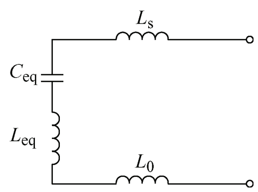

Fig. 4 *LC* equivalent circuit of an MMC

The equivalent converter station capacitance and reactance are

$$\begin{cases} L_{eq} = \dfrac{2}{3} L_{arm} \\ C_{eq} = 6\dfrac{C_{SM}}{N_{SM}} \end{cases} \tag{1}$$

where L_{eq} represents the equivalent converter station inductance; L_{arm} represents the bridge arm inductance; C_{eq} represents the equivalent converter station capacitance; C_{SM} represents the SM capacitance; and N_{SM} represents the number of SMs invested.

During the initial stage of the bipolar short-circuit fault, by analyzing the rising trend of the fault current, the discharge state of the capacitor can be regarded as the process of the DC power supply. Suppose the parameter of the smoothing reactor in series with the DC circuit breaker is 100 mH, then the total series inductance of the equivalent circuit L_T is given as follows

$$L_T = L_{eq} + L_s + L_0 \tag{2}$$

where L_s represents the smoothing reactor inductor; and L_0 represents the MMC series reactor inductor.

Denoting the equivalent DC voltage of the SM in the capacitor discharge stage as U_{SM} and the transmission line current as i_{dc}, the transmission line model can be represented by the combination of R_c, L_0, and $C/2$. Therefore, the cable model of the converter is shown in Fig. 5.

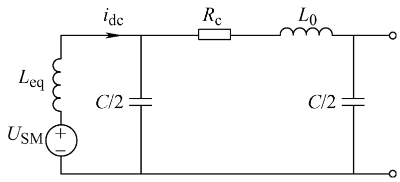

Fig. 5 Model of a converter in the capacitor discharge stage

After the fault occurs, the fault current increases continuously. Meanwhile, the inductance of the faulty line varies accordingly, and direct measurement of the total line inductance during this time becomes difficult. Based on the relationship between line voltage and inductive reactance, we selected the current and voltage values within the first 0.5 ms after the fault began and indicated the single terminal voltage of the line as U_{dc}. Therefore

$$\left|\frac{di_{dc}}{dt}\right|_{t\to 0} = \frac{U_{dc}}{L_T'} \tag{3}$$

The initial rise rate of the fault current (RRC) can be defined as

$$RRC = \left|\frac{di_{dc}}{dt}\right|_{t\to 0} \tag{4}$$

The inductance of fault line can be calculated as follows

$$L_T' = \frac{U_{dc}}{RRC} \tag{5}$$

It can be seen that the line inductance can be indirectly calculated by measuring the rate of rise of voltage and current in real-time, which can be used as the simultaneous total line inductance in series to judge whether a DC fault had occurred. This process only requires the voltage and current values of the line, rather than the information from the remote converter station; this eliminates the requirement for communication channel and reduces the protection time while improving its reliability.

The calculated inductance value of the line obtained from the above process can be used as a reference value for fault identification. Similar to distance protection in traditional AC systems, protection strategies can be formulated based on the inductance of the line in HVDC grids. Accordingly, we installed fault identification protection on both sides of the DC line and set the line inductance from the protection installation to the end of the protection zone as the set inductance value. Furthermore, because this inductance is proportional to the length of the line, when the calculated line inductance is less than the set value, it can detect the occurrence of a fault.

Denoting the fault zone inductance as L_f and the line inductance setting value as L_{set}, we obtain

$$L_f = L_T' - L_{arm} - L_s \tag{6}$$

Moreover, if

$$L_f < L_{set} \tag{7}$$

it indicates that a fault has occurred.

3.3 Simulation and verification

A four-terminal MMC-type HVDC power grid was built in the PSCAD/EMTDC simulation software. Fig. 6 illustrates its simplified topology. Herein, overhead transmission lines were adopted and the main wiring method used a bipolar structure. The positive and negative poles of a DC line are represented in the form of a single line diagram. Specifically, the outflow from the bus is in the positive direction of the current. The system parameters are detailed in Tab. 1. In Fig. 6, F_1 indicates the occurrence of a bipolar short-circuit fault line L_{12}. After the fault is detected, the fault current must be disconnected through the HVDC circuit breaker at two ends of the line to complete the fault isolation and guarantee the normal operation of other sections of the system.

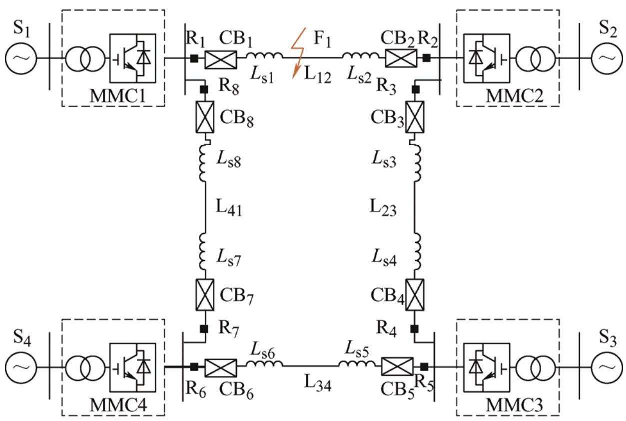

Fig. 6 Four-terminal MMC-HVDC grid

Tab. 1 Parameters of the four-terminal MMC-HVDC grid

Parameter		Value
Line length/km	L_{12}	208
	L_{23}	180
	L_{34}	205
	L_{41}	50
Active power of converter station /MW	Station 1	800
	Station 2	1 000
	Station 3	1 200
	Station 4	500
DC line voltage/kV		±500
Number of SMs on bridge arm		100
SM capacitance/μF		1 000
Smooth wave reactor/mH		100

The simulated system adopted a symmetric bipolar structure similar to the “Zhangbei MT-HVDC Grid Project” and its converter stations implemented a half-bridge MMC topology. In Fig. 6, MMC1 and MMC4 are rectifier stations, MMC2 and MMC3 are inverter stations. Converter stations 1, 3, and 4 adopted the constant active power and constant reactive power control, whereas station 2 employed the constant DC voltage and constant reactive power control [19]. Line protection is installed at R_1-R_8 respectively. Hybrid high-voltage DCCBs labeled CB_1-CB_8 and smooth wave reactors (L_{s1}-L_{s8}) were installed on both sides of the line.

Considering the case when a bipolar short-circuit fault F_1 occurs on L_{12}, the observed rise rate of the fault current through the line is plotted in Fig. 7. It is clear that the fault current is always in the rising state since the occurrence of the fault until the protective device is operated. Variation of the current can be extracted from this graph to calculate its rise rate.

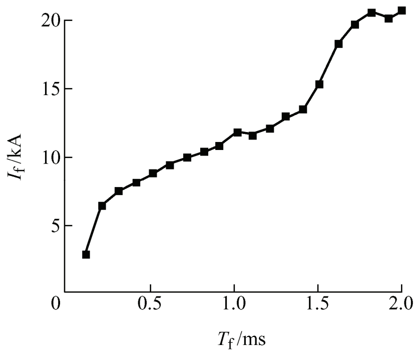

Fig. 7 Line current of bipolar short-circuit fault

Protection devices measure the DC voltage U_{dc} by means of a voltage transformer. During the operation of the system, Eq. (5) can be used to calculate the real-time inductance value L_T' of each converter station. Simulation tests were performed considering bipolar short-circuit faults at different locations to extract fault characteristic quantities at protection distances of 5 km, 10 km, 20 km, 50 km, 75 km, and 100 km. The corresponding inductance values were calculated and compared with the actual inductance values. The results are graphed in Fig. 8. The error analysis involved in this process is obtained using Eq. (8), and the comparison results of these inductance values are provided in Tab. 2.

$$\text{Error rate} = \frac{|L_T - L_T'|}{L_T} \tag{8}$$

It can be summarized from Tab. 2 that the average error between the calculated value and the actual value of the proposed inductance algorithm is maintained at about 4.5%, and the calculation result is relatively accurate, which indicates the feasibility of estimating the line inductance by using the initial rise rate of the current.

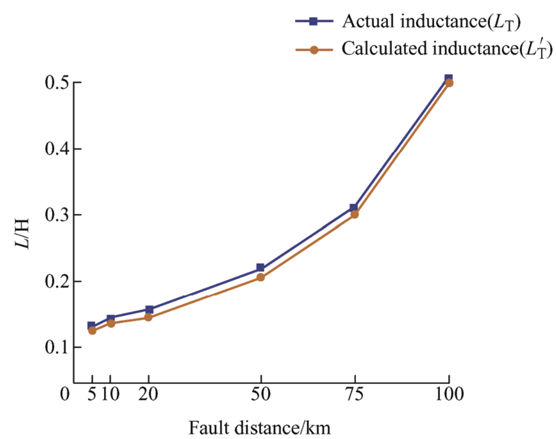

Fig. 8 Actual and calculated inductance at different fault distances

Tab. 2 Comparison between actual and calculated inductance

Inductance	Fault distance/km					
	5	10	20	50	75	100
L_T / H	0.135	0.146	0.162	0.221	0.314	0.506
L_T' / H	0.129	0.141	0.148	0.209	0.302	0.501
Error rate(%)	4.44	3.42	8.64	5.43	3.82	0.99

Furthermore, in the case of a bipolar short-circuit fault, we set different line inductance values ranging between 0-200 mH to simulate the fault current. Fig. 9 illustrates the rise of fault current under these conditions.

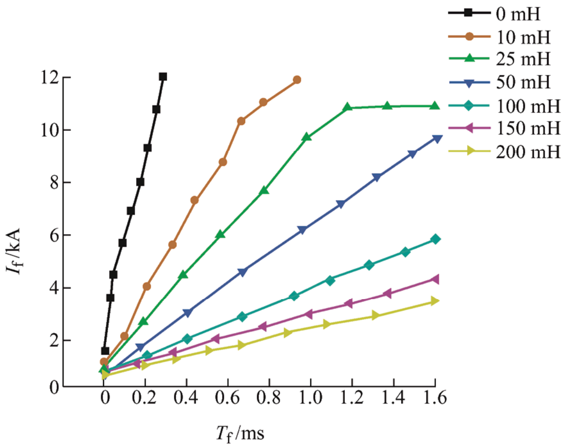

Fig. 9 Fault current with different inductance values for bipolar short-circuit fault

As shown in Fig. 9, when the inductance value in the line is different, the rising amplitude and rise rate of the fault current change simultaneously; moreover, the larger the line inductance value is, the slower the rising rate of the fault current will be. Nevertheless, as long as the calculated inductance is smaller than the set value, a fault is detected.

4 Protection strategy for MT-HVDC DC lines

4.1 Traveling wave protection scheme based on single-ended quantity

Depending on the principle described above, a DC line fault can be detected. This protection strategy can be set as the main protection of the transmission line to ensure real-time and rapid fault monitoring. The HVDC system has an obligation to safeguard the entire line; therefore, it is necessary to distinguish between the inside and outside of the fault zone. At this point, if the implementation of the method that judges the inductance at the local end of the line is continued, the inductances of different transmission lines on the same bus must be compared based on the actual inductance calculated using the voltage and current information, which is slightly defective in determining the speed. Therefore, the principle of traveling wave protection can be introduced as a backup protection to assist the main protection in the previous section and determine the location of the line fault.

In view of the traditional linear traveling wave protection principle, it can be improved to achieve fault section determination and location by using the single-ended traveling wave information collected from the main protection [20-22]. After a short-circuit fault occurs, the fault traveling wave will propagate from the fault point to both ends of the line. Owing to the existence of smoothing reactors, the high-frequency component of this fault traveling wave is limited to the line and does not penetrate into the adjacent lines. Using this feature difference, the short-circuit fault inside and outside the region can be identified. Single-ended travelling wave ranging has better applicability in the case of both transient and permanent faults [23]. The time difference between the single-ended measuring traveling wave's initial arrival at the protection terminal and the reflection from the fault point to the protection terminal is used for distance measurement. Fig. 10a illustrates the fault location schematic diagram of a single-terminal traveling wave. It takes T_1 for the first time when the traveling wave arrives at the end of the line, and T_2 for it to return to it after reflection, with the propagation speed of v. Fig. 10b shows the single-ended traveling wave waveform of the location of the traveling wave protection. The distance from the point of failure to protection is denoted as l_f, and the traveling wave fault location formula can be obtained from the above description as

$$l_f = 0.5(T_2 - T_1)v \tag{9}$$

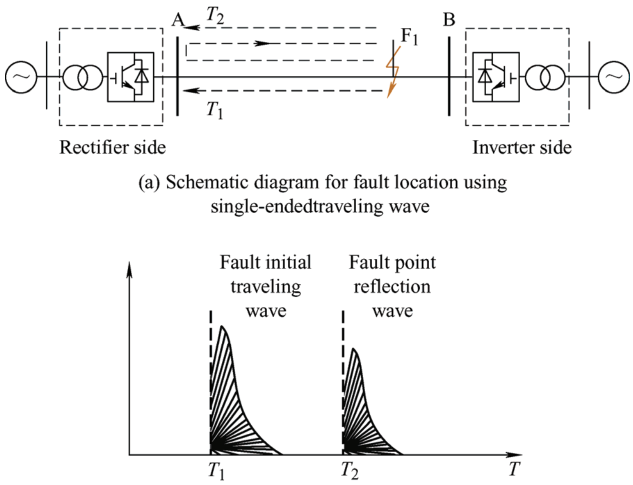

(a) Schematic diagram for fault location using single-endedtraveling wave

(b) Waveform of single-ended fault traveling wave

Fig. 10 Diagram of single terminal traveling wave fault location

The key to traveling wave ranging lies in the reliable detection of traveling waves and the correct calibration of the wave head. After detecting the traveling wave information, the wave head is identified by wavelet decomposition, and the discrete DC wavelet transform is used to obtain the wavelet transform of the collected DC voltage value to complete the fault location [24-25].

4.2 Traveling wave analysis of simulation system

The fault F_1 on line L_{12} in the four-terminal HVDC power grid shown in Fig. 6 is still being considered as an example for this analysis. When a bipolar short-circuit fault occurs, it is an in-zone fault for protection R_1 and an out-of-zone fault for protection R_8, which is another DC line of the same bus. The voltages: forward voltage traveling wave (moving towards the fault point) and backward voltage traveling wave (returning from the fault point), at the two protection points after the fault occurrence were measured and are graphed in Fig. 11.

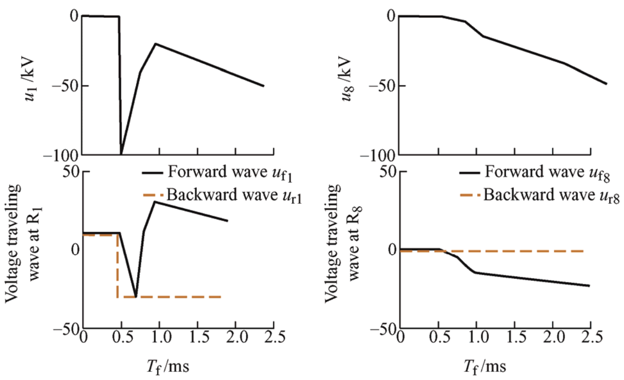

(a) Waveform at R_1 (b) Waveform at R_8

Fig. 11 Diagram of the wave front of traveling wave for bipolar short-circuit fault

Observing the waveforms at these two locations, it can be concluded that the voltage traveling wave of the in-zone fault has a steeper wave head. For out-of-zone faults, the smoothing reactor at the end of the line blocks most of the high-frequency components; consequently, the voltage traveling wave head is relatively gentle. In particular, the reverse voltage traveling wave exhibits negligible change in its waveform, which is quite different from the former. In the same way, for the protection R_2 and R_3 on the adjacent bus lines, it is also possible to determine on which line the fault occurs by extracting the information of the traveling wave head.

Therefore, after a fault occurs on the DC line, only the steepness of the traveling wave head of the reverse voltage at different line protection points needs to be compared to determine whether the faults are in-zone and out-of-zone, thereby realizing the determination of the fault section.

5 Conclusions

In view of the fault characteristics of the MT-HVDC power grid, this paper discusses the DC transmission line fault protection strategy, and proposes a principle of HVDC grid fault monitoring and traveling wave protection based on a single-terminal quantity. The results of theoretical calculation and software modeling simulation indicate the following conclusions.

(1) The novel fault detection principle proposed in this article uses the initial rise rate of the fault current to estimate the line inductance. Through a comparative analysis of the obtained inductance value and the set inductance value, a fault can be detected. This method only needs to extract the single-ended information of the line. Moreover, no communication equipment is needed, and the local information is sufficient for the complete fault monitoring, which ensures the rapidity and reliability of fault protection in addition to improving the actual economics of the project.

(2) In the traveling wave protection scheme designed according to the novel single-terminal fault detection principle, the fault section can be determined only by using the single-terminal traveling wave information. Moreover, the fault location can be determined using the single-terminal traveling wave fault location method. This scheme not only serves as the backup protection of DC line fault, but also coordinates with the single-terminal fault monitoring device in the action sequence, so as to complete the fault detection and location of DC line in a relatively shorter time. This further plays a positive role in the reliable operation of the MT-HVDC power grid transmission system.

References

[1] Z Xu, Q Tu, M Guan, et al. Voltage source converter based HVDC power transmission systems. Beijing: China Machine Press, 2013.

[2] Y Wang, B Zhang, X Fan. Fast protection scheme for

overhead transmission lines of VSC-based HVDC grid. *Automation of Electric Power Systems*, 2016, 40(21): 13-19.

[3] G Cao, K Sun, S Jiang, et al. A modular DC/DC photovoltaic generation system for HVDC grid connection. *Chinese Journal of Electrical Engineering*, 2018, 4(2): 56-64.

[4] C D Barker, A G Adamczyk, R Gupta, et al. Fault clearing on overhead HVDC transmission lines. *Cigre Canada Regional Conference*, September 22-24, 2014, Toronto, Canada.

[5] Q Huang, G Zou, L Gao, et al. Review on DC transmission line protection technologies of HB-MMC based DC grids. *Power System Technology*, 2018, 42(9): 2830-2840.

[6] Y Wu, Z Lu, Z He, et al. Study on the protection strategies of HVDC grid for overhead line application. *Proceedings of the CSEE*, 2016, 36(14): 3726-3734.

[7] B Li, J He, Y Li, et al. Single-ended protection scheme based on boundary characteristic for the multi-terminal VSC-based DC distribution system. *Proceedings of the CSEE*, 2016, 36(21): 5741-5749.

[8] J He, B Li, Y Li, et al. A fast directional pilot protection scheme for the MMC-based MTDC grid. *Proceedings of the CSEE*, 2017, 37(23): 6878-6887.

[9] A Adamczyk, C D Barker, H Ha. Fault detection and branch identification for HVDC grids. *12th IET International Conference Developments in Power System Protection*, March 31-April 3, 2014, Copenhagen, Denmark. IET, 2014: 1-6. DOI: 10.1049/cp.2014.0013.

[10] L Ning, N Tai, X Zheng, et al. Research on MMC-HVDC transmission line protection scheme based on one terminal transient current. *Proceedings of the CSEE*, 2017, 37(17): 5010-5017, 5220.

[11] F Jiang, Y Li, C Tu, et al. A review of series voltage source converter with fault current limiting function. *Chinese Journal of Electrical Engineering*, 2018, 4(1): 36-44.

[12] D Zhou, H Wang, H Wang, et al. Reliability analysis of grid-interfaced filter capacitors. *Chinese Journal of Electrical Engineering*, 2018, 4(3): 21-28.

[13] J Su, J Guo, T Jin. DC fault characteristics and line fault recovery strategy in flexible DC power network. *Transactions of China Electro Technical Society*, 2019, 34(S1): 352-359.

[14] J Hafner, B Jacobson. Proactive hybrid HVDC breakers: A key innovation for reliable HVDC grids. *Proceeding of Cigre Symposium*, September 13-15, 2011, Bologna, Italy.

[15] S Yang, W Xiang, J Wen. Review of DC fault protection methods for the MMC based DC grid. *Proceedings of the CSEE*, 2019, 39(22): 6600-6617.

[16] L Xiao, H Sun, F Gao, et al. A new diagnostic method for winding short-circuit fault for SRM based on symmetrical component analysis. *Chinese Journal of Electrical Engineering*, 2018, 4(1): 74-82.

[17] X Dong, L Tang, S Shi, et al. Configuration scheme of transmission line protection for flexible HVDC grid. *Power System Technology*, 2018, 42(6): 1752-1759.

[18] C A Rojas, S Kouro, M A Perez, et al. DC-DC MMC for HVDC grid interface of utility-scale photovoltaic conversion systems. *IEEE Transactions on Industrial Electronics*, 2018, 65(1): 352-362.

[19] Y Ma. Research on fault analysis and fault current-limiting scheme for VSC-based multi-terminal DC grid. Jinan: Shandong University, 2018.

[20] M Zhang, J He, G Luo, et al. A fault location method for multi-terminal flexible DC power grid based on local information. *Electric Power Automation Equipment*, 2018, 38(3): 155-161.

[21] Z Jiao, Z Wang, X Wang, et al. Protection schemes for distribution lines in DC power grid. *IEEE Innovative on Smart Grid Technologies-Asia (ISGT ASIA)*, Bangkok. Thailand. IEEE PES, 2015: 1-6.

[22] J Zhang, W Xian, H Rao, et al. Research on DC fault protection scheme of overhead MMC based DC grid with DC circuit breaker. *Proceedings of the CSEE*, 2018, 38(16): 4631-4645, 4969.

[23] D Tzelepis, A Dyśko, G Fusiek, et al. Single-ended differential protection in MTDC networks using optical sensors. *IEEE Transactions on Power Delivery*, 2017, 32(3): 1605-1615.

[24] S Li, X Wang, T Li, et al. Optimal design for hybrid MMC and its DC fault ride through strategy. *Proceedings of the CSEE*, 2016, 36(7): 1849-1858.

[25] X Yu, L Xiao, L Lin, et al. Single-ended fast fault detection scheme for MMC-based HVDC. *High Voltage Engineering*, 2018, 44(2): 440-447.

Sihua Wang was born in Jiangsu Province, China, on May 21, 1968. He graduated from the East China Jiaotong University, electrical engineering and automation in Jiangxi, China, in 1995.

He is a professor at Lanzhou Jiaotong University, Lanzhou, China. His research interests concern reliability of substation integrated automation and direction of HV insulation.

Lijun Zhou was born in Gansu Province, China, on August 3, 1996. She is studying for a master's degree in power system and automation at Lanzhou Jiaotong University, Lanzhou, China. Her research interests concern protection and control of HVDC power grid.

Tian Wang was born in Gansu, China, on September 25, 1995. She is studying for a master's degree in electrical engineering at Lanzhou Jiaotong University, Lanzhou, China. Her research interests concern fault monitoring and diagnosis of new energy grid.

Tianyu Chen was born in Zhejiang, China, on October 9, 1995. He is studying for a master's degree in electrical engineering at Lanzhou Jiaotong University, Lanzhou, China. His research interests concern monitoring and control of electrified railway.

Yu Wang was born in Hubei, China, on April 3, 1994. He is studying for a master's degree in electrical engineering at Lanzhou Jiaotong University, Lanzhou, China. His research interests concern overvoltage and lightning protection grounding technology.